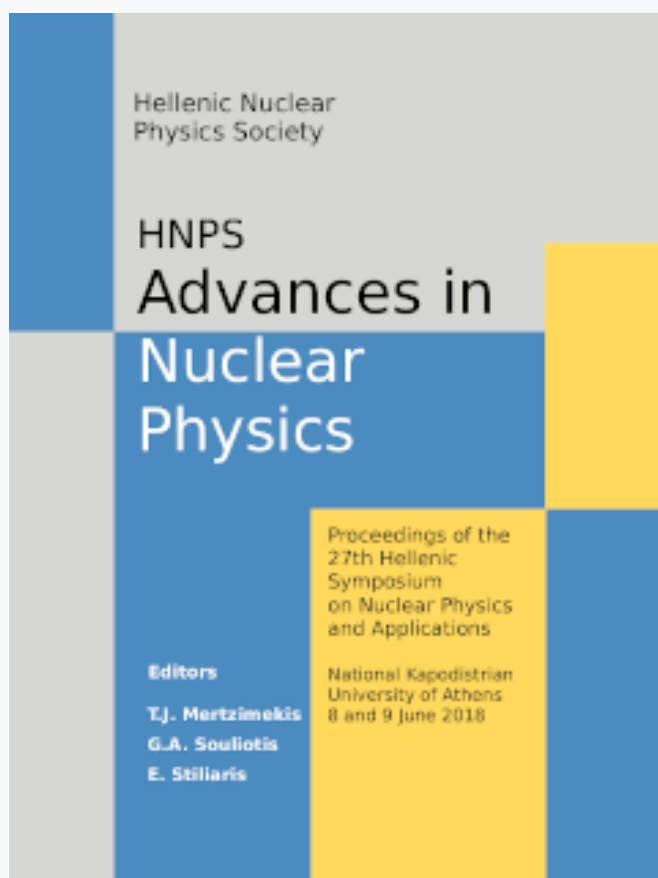


HNPS Advances in Nuclear Physics

Vol 26 (2018)

HNPS2018



Investigation of the C3+ Auger KLL spectrum obtained in collisions of 6-15 MeV C4+ (1s2, 1s2s 3S) with gas targets

I. Madesis, A. Laoutaris, E. P. Benis, T. J. M. Zouros

doi: [10.12681/hnps.1807](https://doi.org/10.12681/hnps.1807)

To cite this article:

Madesis, I., Laoutaris, A., Benis, E. P., & Zouros, T. J. M. (2019). Investigation of the C3+ Auger KLL spectrum obtained in collisions of 6-15 MeV C4+ (1s2, 1s2s 3S) with gas targets. *HNPS Advances in Nuclear Physics*, 26, 125–132. <https://doi.org/10.12681/hnps.1807>

Investigation of the C^{3+} Auger KLL spectrum obtained in collisions of 6-15 MeV C^{4+} ($1s^2$, $1s2s\ ^3S$) with gas targets

I. Madesis^{*1,2}, A. Laoutaris^{1,2}, E.P. Benis³, and T. J. M. Zouros^{1,2}

¹ *Department of Physics, University of Crete, Voutes Campus, GR-70013 Heraklion, Greece*

² *Tandem Accelerator Laboratory, INPP, NCSR Demokritos, GR 15310 Ag. Paraskevi, Greece*

³ *Department of Physics, University of Ioannina, GR 45110 Ioannina, Greece*

Abstract Single electron transfer to the $1s2s\ ^3S$ long-lived component of the naturally occurring mixed-state ($1s^2$, $1s2s\ ^3S$) C^{4+} ion beam in collisions with gas targets was investigated using zero-degree Auger projectile spectroscopy at the Demokritos 5.5 MV tandem accelerator. The observed KLL Auger spectrum contains $1s2s2p\ ^2P$ and 4P states resulting from direct $2p$ transfer to the $1s2s\ ^3S$. Higher lying ($1s2s\ ^3S$) $nl\ ^{2,4}L$ states produced by nl transfer ($n>2$) were also observed and can in principle feed the lower lying $1s2s2p\ ^2P$ and 4P states. However, due to spin selection rules only the quartets have large enough radiative branching ratios resulting in a proposed selective feeding of only the $1s2s2p\ ^4P$ state by E1 cascades, while minimally affecting the $1s2s2p\ ^2P$ states. In the absence of cascades, the ratio of cross sections for $2p$ transfer to the $1s2s\ ^3S$ state, $R_m \equiv \sigma_m(^4P)/\sigma_m(^2P)$, is 2 according to spin statistics. However, the $1s^2$ ground state beam component also contributes to the production of the $1s2s2p\ ^2P$ doublet states by transfer-excitation. To isolate just the $1s2s\ ^3S$ transfer contribution and compute R_m , a new technique was employed requiring the recording of two KLL spectra, with the same collision energy, but each with appreciably different $1s2s\ ^3S$ content, varied by stripping techniques. Our determination of R_m shows this to be >2 , in agreement with spin statistics, but contrary to the expected 4P enhancement due to cascade feeding. Details of the analysis and results are discussed.

Keywords Ion-atom collisions, Zero-degree Auger projectile spectroscopy, Cascade feeding, single electron transfer, mixed-state beams, He-like ions, Li-like ions, KLL Auger.

INTRODUCTION

Using a new technique recently developed by our group [1], we have been able to separate the KLL Auger contributions of just the $1s2s\ ^3S$ metastable component from those of the $1s^2$ ground state component in energetic collisions of mixed state ($1s^2$, $1s2s\ ^3S$) C^{4+} ion beams with gas targets. The $1s2s\ ^3S$ metastable component allows for the formation of doubly-excited $1s2s2p\ ^2P$ and 4P Li-like states by direct $2p$ electron transfer from the target atom, which can be clearly identified in the high resolution Auger KLL spectra obtained with our zero-degree Auger projectile spectroscopy (ZAPS) setup [2-4]. In addition, spin doublets and quartets ($1s2s\ ^3S$) $nl\ ^{2,4}L$, also formed by nl transfer to higher lying states with $n>2$, can be expected to feed the lower lying $1s2s2p\ ^{2,4}P$ states, influencing their ratio. However, as already proposed [5], only the $1s2s2p\ ^4P$ is preferentially populated by such a cascade feeding. The effect of the selective cascade feeding mechanism can possibly be identified by measuring the ratio, $R_m =$

* Corresponding author, email: imadesis@physics.uoc.gr

$\frac{\sigma_m(^4P)}{\sigma_m(^2P_-)+\sigma_m(^2P_+)}$, of the cross sections for the production of $1s2s2p\ ^4P$ and the $1s2s2p\ ^2P_{\pm}$ states by $2p$ transfer to the $1s2s\ ^3S$ component, which should exhibit an enhancement over its spin statistics value of 2 [5].

EXPERIMENTAL DETAILS

The measurements were performed with our ZAPS setup on beamline L45 at the National Center for Scientific Research (NCSR) Demokritos 5.5 MV tandem accelerator facility. The experimental setup, shown in Fig. 1, is composed of a single stage hemispherical deflector analyzer (HDA) with a four-element injection lens and a 2-D position sensitive detector (PSD) combined with a doubly differentially pumped gas target, described in detail in Refs. [2, 3]. The He-like C^{4+} mixed-state beam was delivered at energies between 6 and 15 MeV and directed into a cylindrical gas target cell. Ne and He gas targets were used with typical pressures in the 5 – 20 mTorr range to maintain single collision conditions.

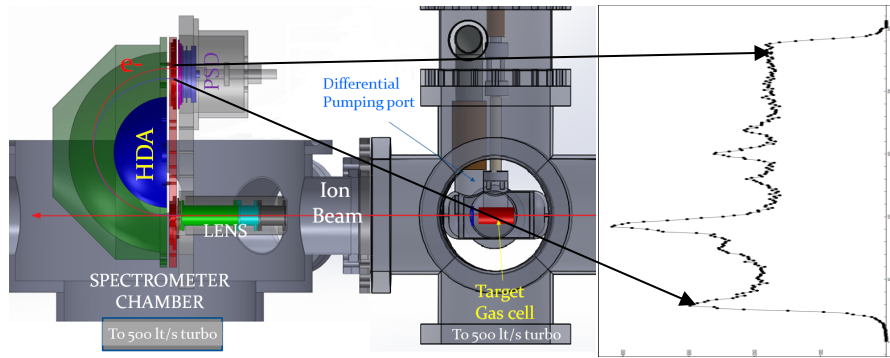


Fig. 1. [Left] The ZAPS experimental setup housed at L45 beamline of the 5.5MV Demokritos tandem. The ion beam (red horizontal arrow) collides with the target gas and traverses the lens and HDA. [Right] Typical high-resolution KLL Auger electron spectrum as recorded by the 2-D PSD.

Carbon Auger electrons emitted at zero-degrees with respect to the beam direction were energetically analyzed by the HDA and recorded with high resolution at the PSD. The electron energy resolution was improved by pre-retardation in the lens [6-8]. Typically, a pre-retardation factor of $F=4$ was adequate to resolve the KLL Auger lines presented here.

He-LIKE PRE-EXCITED IONIC STATES ($1s2s\ ^3S$)

Depending on the energy of the ion beam during the stripping process, a particular Gaussian-like charge state distribution results, centered around the mean charge state. Higher stripping energy leads to a higher mean charge state [9-11]. Thus, to produce more intense few-electron or even bare ion beams, additional stripping points after acceleration, known as post(-acceleration)-strippers, are used. He-like and Be-like ionic beams, are typically delivered in mixed states due to the long lifetime of certain excited ionic states. He-like beams, in particular, are delivered in a mixture of $1s^2\ ^1S$ ground state and $1s2s\ ^3S$ metastable state [12, 13]. The

amount of metastable fraction in the ion beam is determined by the stripping medium's effective areal density, and its distance from the target [12-14].

KLL AUGER ELECTRON SPECTRUM - POPULATING THE $1s2l2l'$ STATES

The observed KLL Auger spectrum originates from the lower-lying doubly-excited C^{3+} states involving a K-vacancy. The five Auger lines that comprise it are shown in the analyzed ZAPS spectrum of Fig. 2. These states are identified in the spectrum as $1s2s^2\ ^2S$, $1s2s2p\ ^4P$, $1s[2s2p\ ^3P]\ ^2P_-$, $1s[2s2p\ ^1P]\ ^2P_+$ and $1s2p^2\ ^2D$. The general reaction is:

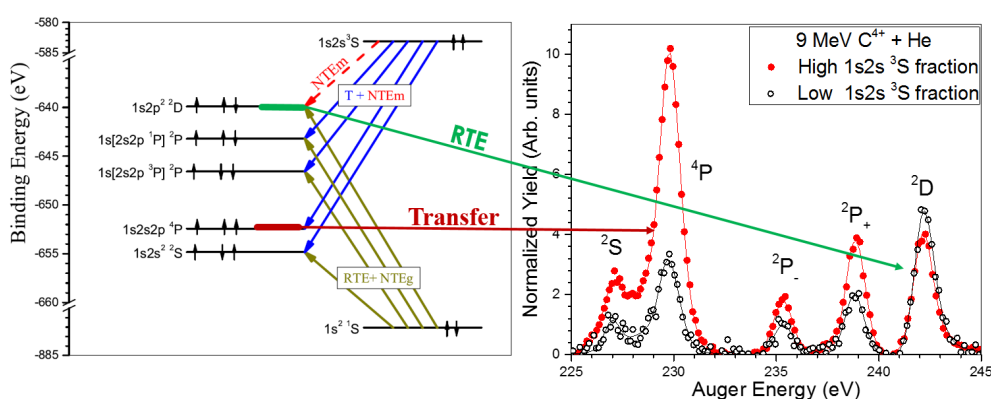
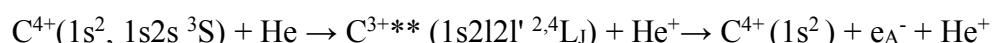


Fig. 2. Carbon Auger KLL lines: [Left] Energy level diagram and corresponding production mechanisms. [Right] Two ZAPS KLL spectra for 9 MeV mixed-state C^{4+} collision with He, each with different metastable content. The intensity of the $1s2s2p\ ^4P$ lines formed by direct $2p$ transfer to the $1s2s\ ^3S$ state is proportional to the metastable beam fraction.

For these KLL states the main production mechanisms as shown in Fig. 2 are:

- **Transfer (T):** In single electron transfer, an electron is transferred from the target to the projectile ion. Although transfer can occur to the $1s^2$ ground state ions, the resulting $1s^2nl$ ($n \geq 2$) states are not autoionizing and therefore not observed. Alternatively, transfer to the $1s2s\ ^3S$ component of the beam leads to the formation of the $1s2snl\ ^{2,4}L_J$ states [5, 15, 16] which Auger decay to the $C^{4+}(1s^2)$ ground state and are recorded by our ZAPS setup.
- **Resonant Transfer and Excitation (RTE):** In RTE [17, 18], a target electron is transferred to the ion, while a projectile electron is excited to a higher-lying level during the same collision, through the electron-electron interaction, in a correlated two-electron process analogous to the time reversed Auger decay [19, 20]. As such, RTE is a resonant process with all the attributes of an Auger transition. Since the $1s2s\ ^3S$ state lies energetically above the respective $(1s2s\ ^3S)nl\ ^{2,4}L$ states it cannot be populated by RTE, since an Auger decay from these states to the $1s2s\ ^3S$ state is not energetically possible. Thus, RTE can only energetically occur from the $1s^2$ ground state component of the ion beam.
- **Non-resonant Transfer and Excitation (NTE):** NTE from the metastable (NTE_m) or ground state (NTE_g) component of the ion beam [21-23] differs from RTE in that both excitation and transfer happen *independently* in the same collision. Projectile excitation is

due to a target nucleus – projectile electron interaction, while transfer due to a projectile nucleus - target electron interaction, both treated as single electron processes. Thus, NTE does not exhibit a resonant behavior similar to RTE. Instead, the interaction strength depends strongly on the projectile velocity, the target nuclear charge and the number of active electrons. Heavy gas targets such as Ne or Ar tend to exhibit larger NTE cross sections, whereas for much lighter H₂ or He targets NTE is much smaller [24].

As shown in Fig. 2, it has been assumed that the 1s2s2p ⁴P level is *solely* populated by 2p transfer to the 1s2s ³S state, while the 1s2p² ²D level is predominantly populated from the 1s² level (both by RTE and NTEg). The population of the 1s2s2p ⁴P from the 1s² component is inhibited by the requirement of a spin-flip, of very low probability for low Z_p ions. These two assumptions, valid in the energy range of 6-15 MeV, particularly for light targets such as H₂ and He, are necessary in the separation of the beam component contributions to the spectra [1]. All other KLL levels are populated from both ground and metastable beam component.

SEPARATING GROUND AND METASTABLE COMPONENT CONTRIBUTIONS

Since the ²P_± and ²S doublets are populated from both beam components, the contributions from each component need to be separately determined. Depending on the energy and the stripping method used, the 1s2s ³S metastable content of the beam can be varied [12, 13]. In particular, a gas terminal stripper (GTS) is known to produce beams with significantly lower metastable content (< 5%) [12-14]. This allowed for the early developments of the two-measurements technique [13], in which however, the low, but non-zero, metastable fraction was assumed *negligible*, with small error. The high metastable content measurement is typically performed with a foil stripper, while the second, much lower metastable content measurement, with a gas stripper [13]. The two KLL spectra were then normalized at the 1s2p² ²D line and subsequently subtracted resulting in just the 1s2s ³S contributions [13,16]. In the more recent improved technique [1], the condition of a zero metastable fraction in the low fraction second measurement can be relaxed, as long as the two fractions are appreciably different. This is particularly helpful in cases where the production of a low enough metastable fraction is not always possible [1, 25]. However, the two assumptions that: a) the 1s2s2p ⁴P state is exclusively populated from the 1s2s ³S component and, b) the 1s2p² ²D state is exclusively populated from the 1s² ground state must still remain. The two metastable fractions can then be directly determined and the spectral contributions of each beam component can be extracted as well [1]. Moreover, the determination of the ratio R_m is facilitated, as there is no need to first explicitly determine the metastable fractions. Instead, R_m is given by the following equation [1]:

$$R_m \equiv \frac{\left(\frac{N_1^e[{}^4P]}{N_1^e[{}^2D]} - \frac{N_2^e[{}^4P]}{N_2^e[{}^2D]} \right) \frac{1}{G_\tau \xi[{}^4P]}}{\left(\frac{N_1^e[{}^2P_+]}{N_1^e[{}^2D]} - \frac{N_2^e[{}^2P_+]}{N_2^e[{}^2D]} \right) \frac{1}{\xi[{}^2P_+]} + \left(\frac{N_1^e[{}^2P_-]}{N_1^e[{}^2D]} - \frac{N_2^e[{}^2P_-]}{N_2^e[{}^2D]} \right) \frac{1}{\xi[{}^2P_-]}}$$

The subscripts 1 and 2 denote either of the two measured KLL spectra, e.g. $N_1^e[{}^4\text{P}]$ denotes the electron yield of the ${}^4\text{P}$ line in the first spectrum. $\xi[x]$ denotes the Auger yield for the state x and G_τ is the solid angle correction factor for the $1s2s2p$ ${}^4\text{P}$, discussed in the next section. The main advantage of this approach is that R_m is computed as a ratio of line intensity ratios of the *same* spectrum. Any absolute normalization parameters, thus cancel [1, 25], allowing for a more accurate determination of R_m .

EFFECTIVE SOLID ANGLE – THE CORRECTION FACTOR G_τ

The state $1s2s2p$ ${}^4\text{P}_J$ is also metastable with lifetimes of the order of 1-120 ns, depending on the value of its J-component [26]. Due to the particular geometric arrangement of the ZAPS setup, the metastable ${}^4\text{P}$ state Auger decays all along the path of the ion beam resulting in a loss of Auger electrons for decays inside and beyond the HDA, as well as in an increase of the solid angle for decays much closer to the HDA [13, 15, 16, 26-28]. To find the appropriate correction for these two competing effects and to also incorporate possible additional filtering by the entry lens, the ion optics package SIMION [29] was utilized. The apparatus was modelled within the SIMION design environment. A weighted distribution of electron emission points along the ion path was defined for every combination of J-component and projectile energy. A Monte Carlo approach was then used, with the detected electron distributions compared to those of a prompt state (lifetime ~ 10 fs). Remarkable agreement between the simulated and the experimental line shapes for the ${}^4\text{P}$ was found [28]. Statistical averaging of the J-component resulted in a correction factor G_τ for each projectile energy. To further verify these simulations, an additional experimental approach was also used as a cross check [30, 31]. Since C^{2+} ion beams in the $1s^22s2p$ ${}^3\text{P}$ metastable state in collisions with H_2 are known to lead to $1s$ *needle* ionization [32] (i.e. the removal of a K-shell electron without affecting the surrounding electrons), the populations of the ${}^4\text{P}$ to ${}^2\text{P}$ states can be shown to result in the ratio of 2:1, from which the correction factor G_τ can be determined [31]. A particular advantage of this newly proposed experimental determination of G_τ is that the produced $1s2s2p$ ${}^4\text{P}$ state is free of any cascade contributions which might complicate its determination. Fair agreement between SIMION and experiment was found [31].

CASCADE FEEDING OF THE ${}^2,{}^4\text{P}$ STATES

As already mentioned, transfer to the $1s2s$ ${}^3\text{S}$ metastable state of the projectile can also populate a variety of $(1s2s$ ${}^3\text{S})nl$ ${}^2,{}^4\text{L}$ configurations with $n > 2$. As seen in Fig. 3, these higher-lying doubly-excited levels can be divided into two distinct spin types: doublets and quartets. For the quartets, Auger decay to the ground state is very weak, as it implies a violation of the spin conservation rule requiring a spin-orbit/-other-orbit interaction with orders of magnitude smaller relative transition rates ($\sim \alpha^4$) [33]. Competing radiative E1 transitions between quartets (red arrows in Fig. 3) are much stronger and prevail. Thus, the quartets preferentially decay in a cascade sequence of E1 transitions, eventually leading to the accumulation of all higher-lying

quartet populations into the $1s2s2p\ ^4P$ state [5, 27, 34-36], which therefore acts as a kind of ground state for all $1s2snl\ ^4L$ decays. For the doublets, however, the Auger decay channel is much stronger than the competing radiative channels, at least for low- Z_p elements, such as carbon [4, 37, 38]. Therefore, the higher-lying doublet states, will mostly Auger decay with minimal cascade feeding of the lowest 2P states [36] with Auger energies between 270 and 298 eV [38], as already observed in our spectra. Assuming the ratio R_m is 2 due to spin statistics, as proposed in Refs. [5, 15, 39], then the additional selective cascade feeding of the $1s2s2p\ ^4P$ should result in an enhancement of R_m above 2. In Fig. 4, experimental results for the R_m ratio are presented for 6, 9, 12 and 15 MeV collisions of C^{4+} with He and Ne. R_m is seen to be very close to the spin statistics value of 2, in contradiction to the expected enhancement due to selective cascade feeding.

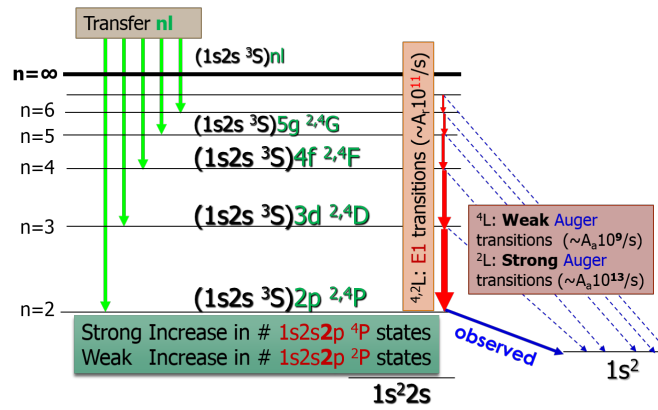


Fig. 3. Cascade feeding of states populated by transfer to the $1s2s\ ^3S$ component. The higher-lying *quartets* decay radiatively by strong E1 transitions since competing Auger decays are weak due to spin conservation considerations. In contrast, for the *doublets*, Auger decay is stronger than the competing E1 transitions, eventually leading to a preferential enhancement of the $1s2s2p\ ^4P$ population.

RESULTS AND DISCUSSION

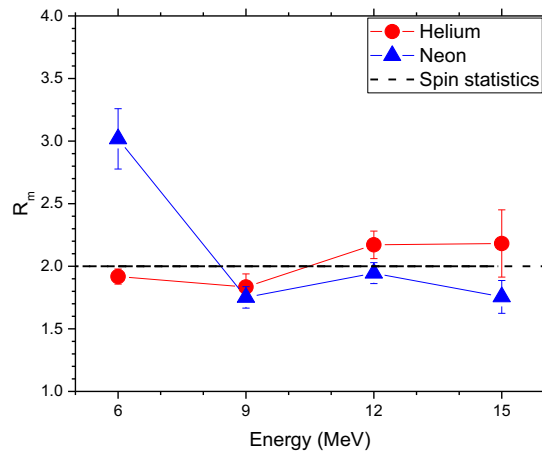


Fig. 4. Experimental results on the ratio R_m of $1s2s2p\ ^4P$ to 2P cross sections for transfer to the metastable component as a function of the C^{4+} collision energy.

Clearly, our results shown in Fig. 4, are unexpected, particularly in the case of He. Previous experimental measurements of R_m [16], showed a higher value, around 6-8, for both He and Ne, while theory including cascades showed values between 4 and 5 [36]. However, the larger experimental results [16] can most likely be traced to incorrect determination of the effective solid angle correction factors G_τ [31]. Applying our simulation method to the setup of Ref. [16], their geometrical correction factors were recalculated [31], resulting in lower corrected R_m values close to 2, in agreements with our results.

As seen in Fig. 4, for He, R_m is very close to 2, well within experimental uncertainties, over the range of measured energies. A slight energy dependence resulting in increasing R_m values with increasing collision energy is also observed, similar to the one seen in Ref. [36]. These two results are puzzling since a value of 2 indicates a possible *absence* of the expected cascades [5, 36] for the 4P , while the energy dependence of R_m goes contrary to the expected increased transfer cross sections (and therefore cascade feeding) at lower collision energies [5]. For Ne the picture is probably more complicated. At 6 MeV a measurable increase is observed, while for the rest of the energies results are similar to those of He. The Ne target, however, although used in similar experiments [16], is probably not the best choice for two basic reasons: Firstly, its electron structure is rather complicated both in terms of transfer and RTE calculations, where contributions from various orbitals require weighting. Secondly, Ne gives rise to much larger NTEM contributions, possibly not satisfying the aforementioned criteria necessary for the separation of the contributions.

SUMMARY AND CONCLUSIONS

A series of ZAPS measurements of 6-15 MeV C^{4+} ($1s^2, 1s2s\ ^3S$) collisions with He and Ne has been performed and preliminary results were presented. The KLL Auger electron contributions resulting from electron transfer to the $1s2s\ ^3S$ component were extracted using our new two-measurement method. The experimentally determined value of $R_m \simeq 2$ seems to indicate an agreement with spin statistics and an absence of cascade feeding of the $1s2s2p\ ^4P$ state in blatant contradiction to expectations. Clearly, further work is required. Future plans include new isoelectronic measurements on other He-like ions and explicit theoretical calculations of all discussed processes including a detailed cascade analysis.

ACKNOWLEDGEMENTS

This research was funded by the APAPES grant covering the period 2012-2015 and the CALIBRA grant covering the period after 2017. Specific acknowledgments read as follows: *APAPES (2012-2015)*: This research has been co-financed by the European Union (European Social Fund ESF) and Greek national funds through the Operational Program "Education and Lifelong Learning" of the National Strategic Reference Framework (NSRF) Research Funding Program: THALES. Investing in knowledge society through the European Social Fund, grant number MIS 377289. *CALIBRA/EYIE (2017-2021)*: We acknowledge support of this work by the project "Cluster of Accelerator Laboratories for Ion-Beam Research and Applications -

CALIBRA” (MIS 5002799) which is implemented under the Action “[Reinforcement of the Research and Innovation Infrastructure](#)”, funded by the Operational Programme "Competitiveness, Entrepreneurship and Innovation" (NSRF 2014-2020) and co-financed by Greece and the European Union (European Regional Development Fund).

REFERENCES

- [1] E. P. Benis and T. J. M. Zouros, *J. Phys. B* **49**, 235202 (2016)
- [2] I. Madesis *et al.*, *J. Phys: Conf. Ser.* **583**, 012014 (2015)
- [3] A. Dimitriou *et al.*, *J. Atom. Mol. Cond. Nano Phys.* **3**, 125 (2016)
- [4] T. J. M. Zouros and D. H. Lee, in *Accelerator Based Atomic Physics Techniques and Applications*, edited by S. M. Shafroth and J. C. Austin (American Institute of Physics Conference Series, Woodbury, NY, 1997), Chapter 13, pp. 426–479
- [5] T. J. M. Zouros, B. Sulik, L. Gulyas, and K. Tökési, *Phys. Rev. A* **77**, 050701 (2008)
- [6] T. J. M. Zouros and E. P. Benis, *J. Electron Spectrosc. and Relat. Phenom.* **125**, 221 (2002)
- [7] T. J. M. Zouros and E. P. Benis, *J. Electron Spectrosc. and Relat. Phenom.* **142**, 175 (2005)
- [8] E. P. Benis and T. J. M. Zouros, *J. Electron Spectrosc. and Relat. Phenom.* **163**, 28 (2008)
- [9] H. D. Betz, *Rev. Mod. Phys.* **44**, 465 (1972)
- [10] R. Sayer, *Rev. Phys. Appl. (Paris)* **12**, 1543 (1977)
- [11] A. Laoutaris *et al.*, *J. Phys: Conf. Ser.* **635**, 052062 (2015)
- [12] M. Zamkov, E. P. Benis, P. Richard, and T. J. M. Zouros, *Phys. Rev. A* **65**, 062706 (2002)
- [13] E. P. Benis, M. Zamkov, P. Richard, and T. J. M. Zouros, *Phys. Rev. A* **65**, 064701 (2002)
- [14] E. P. Benis *et al.*, *Nucl. Instrum. Methods Phys. Res. B* **205**, 517 (2003)
- [15] J. A. Tanis *et al.*, *Phys. Rev. Lett.* **92**, 133201 (2004); *ibid.* **96**, 019901 (2006)
- [16] D. Strohschein *et al.*, *Phys. Rev. A* **77**, 022706 (2008)
- [17] J. A. Tanis *et al.*, *Phys. Rev. Lett.* **49**, 1325 (1982)
- [18] D. Brandt, *Phys. Rev. A* **27**, 1314 (1983)
- [19] M. Schulz *et al.*, *Phys. Rev. A* **38**, 5454 (1988)
- [20] M. Schulz *et al.*, *Phys. Rev. Lett.* **62**, 1738 (1989)
- [21] D. Brandt, *Nucl. Instrum. Methods* **214**, 93 (1983)
- [22] P. L. Pepmiller *et al.*, *Phys. Rev. A* **31**, 734 (1985)
- [23] J. K. Swenson *et al.*, *Phys. Rev. Lett.* **57**, 3042 (1986)
- [24] T. J. M. Zouros *et al.*, *Phys. Rev. A* **40**, 6246 (1989)
- [25] E. P. Benis, S. Doukas, T. J. M. Zouros, *Nucl. Instrum. Methods Phys. Res. B* **369**, 83 (2016)
- [26] E. P. Benis *et al.*, *Nucl. Instrum. Methods Phys. Res. B* **365**, 457 (2015)
- [27] T. J. M. Zouros, B. Sulik, L. Gulyas, and A. Orban, *J. Phys. B* **39**, L45 (2006)
- [28] S. Doukas *et al.*, *Rev. Sci. Instrum.* **86**, 043111 (2015)
- [29] <http://www.simion.com>
- [30] D. H. Lee *et al.*, *Phys. Rev. A* **46**, 1374 (1992)
- [31] E. P. Benis *et al.*, *J. Electron Spectrosc. and Relat. Phenom.* **222**, 31 (2018)
- [32] N. Stolterfoht *et al.*, *Nucl. Instrum. Methods Phys. Res. B* **24/25**, 168 (1987)
- [33] P. Feldman and R. Novik, *Phys. Rev.* **160**, 143 (1967)
- [34] S. M. Younger and W. L. Wiese, *Phys. Rev. A* **17**, 1944 (1978)
- [35] R. Mann, *Phys. Rev. A* **35**, 4988 (1987)
- [36] D. Röhrbein, T. Kirchner, and S. Fritzsche, *Phys. Rev. A* **81**, 042701 (2010)
- [37] N. Stolterfoht, *Physics Reports* **146**, 315 (1987)
- [38] M. H. Chen, *At. Data & Nucl. Data Tables* **34**, 301 (1986)
- [39] E. P. Benis *et al.*, *Phys. Rev. A* **73**, 029901 (2006)